Pure appl. geophys. 164 (2007) 2271–2290
0033–4553/07/112271–20
DOI 10.1007/s00024-007-0272-x

Pure and Applied Geophysics

Multifractal Analysis of Earthquakes in the Southeastern Iran-Bam Region

P. N. S. Roy[1] and Amit Padhi[2]

Abstract—Earthquakes in Iran and neighbouring regions are closely connected to their position within the geologically active Alpine-Himalayan belt. Modern tectonic activity is forced by the convergent movements between two plates: The Arabian plate, including Saudi Arabia, the Persian Gulf and the Zagros Ranges of Iran, and the Eurasian plate. The intensive seismic activity in this region is recorded with shallow focal depth and magnitude rising as high as $M_w = 7.8$. The study region can be attributed to a highly complex geodynamic process and therefore is well suited for multifractal seismicity analysis. Multifractal analysis of earthquakes ($m_b \geq 3$) occurring during 1973 – 2006 led to the detection of a clustering pattern in the narrow time span prior to all the large earthquakes: $M_w = 7.8$ on 16.9.1978; $M_w = 6.8$ on 26.12.2003; $M_w = 7.7$ on 10.5.97. Based on the spatio-temporal clustering pattern of events, the potential for future large events can be assessed. Spatio-temporal clustering of events apparently indicates a highly stressed region, an asperity or weak zone from which the rupture propagation eventually nucleates, causing large earthquakes. This clustering pattern analysis done on a well-constrained catalogue for most of the fault systems of known seismicity may eventually aid in the preparedness and earthquake disaster mitigation.

Key words: Fractal, multifractal, geodynamics and seismicity.

1. Introduction

The spatial multifractal dimension (D_q) provides a quantitative measure of spatial clustering and a measure of crustal deformation in space and time of events, indicating the seismicity of a region (Aki, 1981, 1984; King, 1983; Turcotte, 1986; Ito and Matsuzaki, 1990; Main, 1996; Legrand *et al*., 1996; Önçel and Wilson, 2002, 2004, 2006; Nakaya and Hashimoto, 2002; Roy and Ram, 2006). In such systems the numbers of fractures that are larger than a specified size are related by a power law to the size. The physical laws governing the fractal structures are scale-invariant in nature. The occurrence of earthquakes is causally related to the fractures which have fractal structure in their space, time and magnitude distributions. The fractal structures may have either homogeneous or multiscaling characteristics. In recent times, many physical quantities have been considered that do not obey conventional scaling laws. Fractal dimensions

[1] Department of Applied Geophysics, Indian School of Mines University, Dhanbad 826 004, Jharkhand, India. E-mail: pns_may1@yahoo.com
[2] Department of Geology and Geophysics, Indian Institute of Technology, Kharagpur 721 302, W.B., India.

provide a quantitative measure of the spatial clustering of epicentres and also of the seismicity of a region. Generally speaking, a fractal distribution means that there is invariance of scale, that the generating process has a high level of recursion and that the phenomenon is able to cover the embedding space in a certain amount given by the fractal dimension. Moreover, it is possible to determine if the fractal set is homogeneous by measuring its multifractal dimension, D_q. The fractal sets showing multiscaling are heterogeneous and are called multifractal sets. Most fractals in nature are heterogeneous (STANLEY and MEAKIN, 1988; MANDELBROT, 1989). Such fractals are characterized by a generalized dimension D_q, where q takes value as 0,1,2, etc. Details on the (multi) fractal formalism are outlined below. A multifractal correlation-dimension analysis has been performed, with q values ranging from 2 to 22. The value $q = 0$ corresponds to the box-counting fractal dimension itself. Multifractality reflects non-homogeneity of distribution: The greater the difference between the various dimensions D_q, the less homogeneous the distribution. In two dimensions, values of D_q ($q = 0,1,2,...$) near *2* signify a uniform coverage of the plane. Uniform distributions (objects) that are scale-invariant (self-similar) are called fractal (all D_q equal among themselves and equal to D_0). The fractal (correlation) dimension of earthquake epicentres of the Tohoku region, Japan has been estimated by HIRATA (1989), who found that this fractal dimension changes during the seismic cycle. Even the experimentally analysed micro-fracturing fractal nature of a series of 29 granite samples demonstrated that the fractal dimension decrease can be used as a predictor of rock failure (FENG and SETO, 1999).

Earthquakes in Iran and neighbouring regions (e.g., Turkey and Afghanistan) are closely connected to their position within the geologically active Alpine-Himalayan belt. Modern tectonic activity is forced by the convergent movements between two plates: The Arabian plate, including Saudi Arabia, the Persian Gulf and the Zagros Ranges of Iran, and the Eurasian plate that incorporates Europe, Central and East Asia, as well as the interior of Iran. The Iranian plateau accommodates the 35 mm/yr convergence rate between the Eurasian and Arabian plates by strike-slip and reverse faults with relatively low slip rates in a zone 1000 km across (BERBERIAN and YEATS, 1999). The major zones of mobility in decreasing order of activity are, Hindukush, Zagros, Elborz, Chaman fault system, east-central Iran, and the Caucasus and eastern Turkey. The most conspicuous aseismic block is that of western Afghanistan, but smaller blocks in central Iran, Azarbayejan, and the southern Caspian Sea also show noticeable stability (SHOJA-TAHERI and NIAZI, 1981). In this study we have selected the region around Bam in southeast Iran as our analysis domain shown in Figure 1.

Bam lies within the western of two north-south, strike-slip fault systems located on each side of the aseismic Lut desert which together accommodate the relative motion between central Iran and Afghanistan, part of the Eurasian plate (TALEBIAN *et al.*, 2004). The town lies to the east of the Gowk fault on which several large earthquakes have occurred over the past 23 years. The Gowk fault zone, a predominantly right lateral strike-slip zone that extends from 50 km west of Bam northward (WALKER and JACKSON, 2002), has also been associated with several large historical earthquakes.

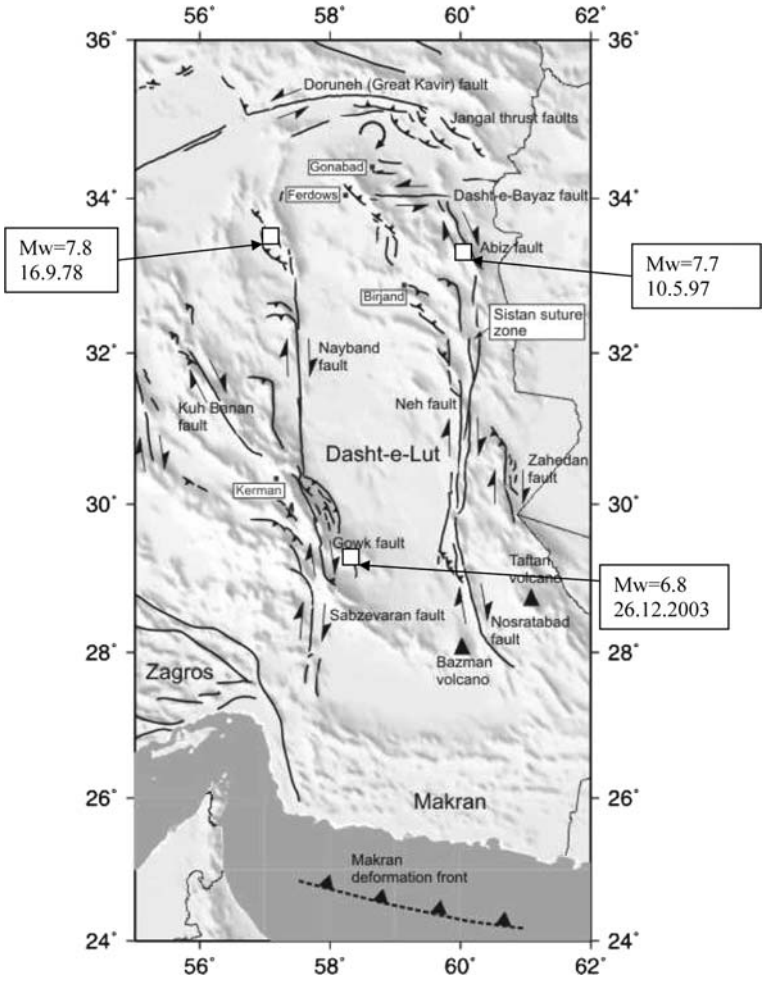

Figure 1
The map of the study region showing major faults in southeastern Iran and the large events considered for the analysis. (after WALKER and JACKSON, 2002).

In the present study, a correlation integral method (GRASSBERGER and PROCACCIA, 1983) is exercised on a catalogue of earthquakes to determine correlation-dimension and generalized fractal dimension. Initially temporal variations of D_C, we prefer to term "statistical precursor" done by considering thirty events' a consecutive windows for the southeastern Iran region. Spatio-temporal study of the events led us to detect a significant drop in D_C values with respect to time prior to a large earthquake. Initial study has helped in detecting the precursor for large earthquakes. Later each large event is taken separately to study its multifractal spatial distribution which leads to the detection of a highly stressed region prior to the main shock.

2. Method

In the present study correlation integral method (GRASSBERGER and PROCACCIA, 1983) is exercised on a catalogue of earthquakes to determine correlation-dimension. A "unique finger print" of a multifractal object requires the introduction of an infinite hierarchy of fractal dimensions, known as generalized fractal dimensions as given below

$$D_q = \{1/(q-1)\}\underset{r\to 0}{\mathrm{Lim}}\left[\log_{10}\left(\sum_i \{P_i(r)\}^q\right)\Big/\log r\right], \tag{1}$$

where D_q exhibits a non-trivial scaling behavior for different values of $q = 1, 2, 3, ...$, $P_i(r)$ is the probability that the events fall into a square box of length r. This phenomenon was described for the first time by MANDELBROT (1989) in the context of fully developed turbulence. Today, it is known as *multifractality*. The original meaning of *multifractal* leads to the question regarding the processes that create multifractal structures. Usually *multi*plicative cascades of random processes generate *multi*fractal structures, while additive processes generally produce simple fractals (*monofractals*) (BUNDE *et al.*, 1990).

Using equation (1), one readily finds the previously defined fractal dimensions for integer q as special cases. The capacity-dimension, the information-dimension, and the correlation-dimension are obtained from

$$\text{Capacity Dimension} = \underset{q\to 0}{\mathrm{Lim}}\, D_q = D_0 \tag{2a}$$

$$\text{Information Dimension} = \underset{q\to 1}{\mathrm{Lim}}\, D_q = D_1 \tag{2b}$$

$$\text{Correlation Dimension} = \underset{q\to 2}{\mathrm{Lim}}\, D_q = D_2 = D_C. \tag{2c}$$

The generalized dimension D_q is defined for all real q and is a monotonically decreasing function of q. There is a lower and an upper limiting dimension $D_{-\infty}$ and D_{∞} respectively, which relate to the regions of the set, in which the measure is "most dilute" and "most dense", respectively.

In two dimensions, values of D_q approaching a value of *2* signify a uniform coverage of the plane. Uniform distributions of events (objects) that are scale-invariant (self-similar) are termed monofractal.

In this paper, the spherical triangle method has been used to determine the distance between the two epicentres (TEOTIA *et al.*, 1997; ÖNÇEL and WILSON, 2002; MANDAL *et al.*, 2005). The correlation integral approach has been employed to compute the correlation dimension and generalized fractal dimension. The methodology to obtain the D_c and D_q are given in details as following:

2.1. (i) Correlation Dimension

The fractal correlation dimension is derived from the correlation integral (GRASSBERGER and PROCACCIA 1983; HILAROV, 1998; ROY and RAM, 2006), which is a cumulative correlation function that measures the fraction of points in the two-dimensional space and is defined as

$$C(r) = \frac{2}{N(N-1)} \sum_{j=1}^{N} \sum_{i=j+1}^{N} H\left(r - r_{ij}\right), \tag{3}$$

where N (for 50-event windows, N will be ${}^{50}C_2$ i.e., 1225 and for 30-event windows N will be ${}^{30}C_2$ i.e., 435) is the total number of pairs in the fractal set to determine D_C, r is the length scale, r_{ij} the distance between the points of a set, which is obtained through the spherical triangle method explained above, H is the Heaviside step function. Therefore, $C(r)$ is proportional to the number of pairs of points of the fractal set separated by a distance less than r. If the system of points examined is a fractal set, the graph of $C(r)$ in logarithmic coordinates must be a linear function with slope D_C equal to the fractal dimension of the system. The graph of $C(r)$ at different stages of the fracture process is shown in Figure 2 (a). The curves show a clear self-similar behavior in a wide range of about two orders of magnitude on the space scale. Deviations from linear dependence in the range of large scales are connected with the finite size of samples, while the other deviation in the range of small scales reflects the boundary effect of data for the region of investigation.

The D_C value is inversely related to the degree of clustering and it requires a higher degree of accuracy in both space and time of the occurrence of events as the present analysis depends on the spatio-temporal distribution of earthquake sequences. In the present analysis an attempt is made to use the catalogue for the earthquakes of the southeastern Iran region, keeping the completeness of the catalogue (WIEMER and WYSS, 2000) in mind. Thus the events of magnitude $m_b \geq 3$ have been considered. It is standard practice to consider the completeness magnitude as the threshold for any analysis that uses a well constrained earthquake catalogue prohibiting error due to presence of a low magnitude earthquake in the region. In the present analysis, wherein we attempted D_c computation which is dependent on the clustering of events. The completeness magnitude may not play a decisive role due to the fact that the catalogue under consideration is expected to have digitally recorded events up to event ≥ 3 (post 1964 WWSN) may be an example. Prohibiting magnitude between 3 and 4 will hypothetically remove a good chunk of data, which would have played a very important role in deciding the energy buildup in the system in the look-out of the zone of extreme stress buildup as a slow process for nucleating a strong event. Since the Gutenberg-Richter relation in itself is not used in the present analysis where b-value is not a parameter considered in relation to D_c. The completeness magnitude is not expected to change the correlation dimension formulation in the search of the numerical precursor. Even ÖNÇEL and WILSON (2002, 2006); NAKAYA and HASHIMOTO (2002); ROY and RAM (2006) did not specify completeness in their studies. However, the improvement of station coverage for obtaining a complete

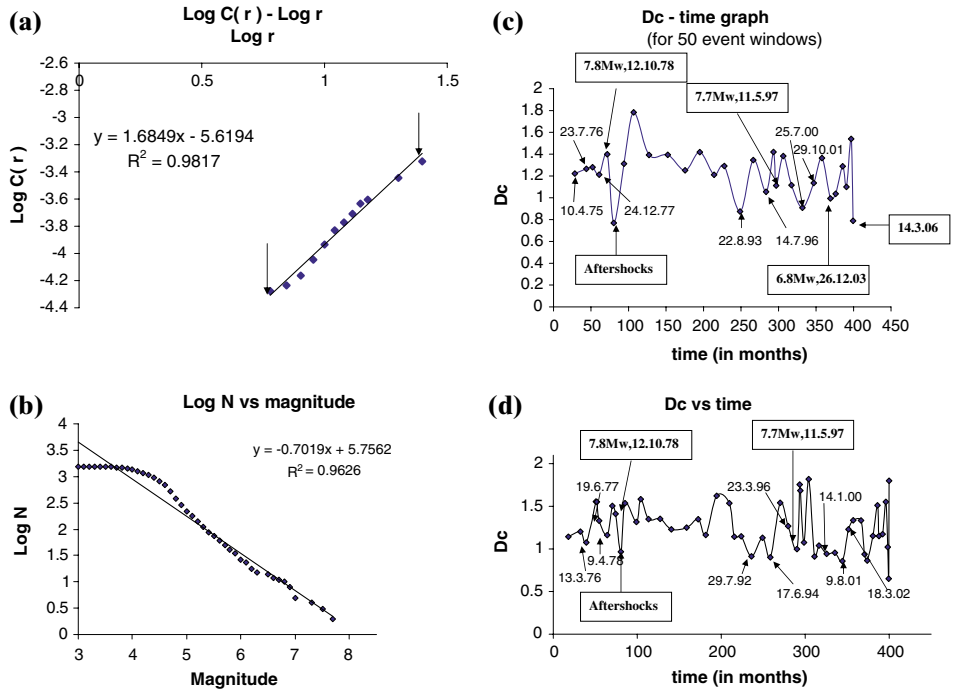

Figure 2

(a): Log $C(r)$ versus Log r is shown for the first time window of thirty events with latitude (24° N – 34° N) and longitude (54° E – 64° E), the slope gives D_C. Arrows demarcate the scaling region obeying power law, i.e., scale invariance. R^2 represents correlation coefficients of the regression line. (b): Plot for frequency magnitude (Gutenberg-Richter) of events ($m_b \geq 2.8$) from 01.01.1973 to 22.05.2006 for the latitude (24° N–34° N) and longitude (54° E – 64° E) showing the completeness of the catalogue of the region. (c): The temporal variation of D_C is shown, where the point (10.4.75), (23.7.76) and (24.12.77) represents significant clustering of events before the main shock of 16.9.1978 ($M_w = 7.8$) for the latitude (24° N – 34° N) and longitude (54° E – 64° E) while considering windows of 50 events each. The plot also shows precursors to the event of 10.5.1997 ($M_w = 7.7$) and the event of 26.12.2003 ($M_w = 6.8$). (d): The temporal variation of D_C is shown, where the point given (13.3.76), (19.6.77) and (9.4.78) represents significant clustering of events before the main shock of 16.9.1978 ($M_w = 7.8$) for the latitude (24° N – 34° N) and longitude (54° E – 64° E) while considering windows of 30 events each. The plot also shows precursors to the event of 10.5.1997 ($M_w = 7.7$) and the event of 26.12.2003 ($M_w = 6.8$).

catalogue will be helpful for efficient forecasting of future events with this technique (Önçel *et al.*, 1995). Again, performance cannot be improved by removing lower magnitude events at the cost of constraining the completeness magnitude of the catalogue as the lower threshold.

2.2. (ii) Generalized Dimension

The multifractal dimension D_q is a parameter representing the complicated fractal structure or multi-scaling nature. The general methods of calculating D_q, are the fixed-mass

method, the fixed-radius method and the box-counting method (MANDELBROT, 1989; GRASSBERGER and PROCACCIA, 1983; HALSEY *et al*., 1986). In the present case, the extended G-P method has been used, which can recover the dimension from a time series (GRASSBERGER and PROCACCIA, 1983; PAWELZIK and SCHUSTER, 1987). Its formula is:

$$\log C_q(r) = D_q \log r (r \to 0), \tag{4a}$$

$$C_q(r) = \left\{ 1/N \sum_{j=1}^{N} \left[(1/N) \sum_{i=j}^{N} H\left(r - \left|X_i - X_j\right|\right) \right]^{q-1} \right\}^{\{1/(q-1)\}}, \tag{4b}$$

where $C_q\,(r)$ = the q-th order correlation integral; $H = a$ Heaviside step function; $r =$ the scaling radius; (for 50-event windows, N will be ${}^{50}C_2$ i.e., 1225) is the total number of pairs in the fractal set to determine D_q; X_i, X_j = the epicentre (given in latitude and longitude) of the i-th event; $|\,X_i - X_j\,| =$ the distance for a given q. In the graph log r-log $C_q\,(r)$, D_q is the slope of the linear segment (i.e., scaling region) as shown in Figures 4 (a)–(h). Similarly, many D_q values can be calculated in the above method for other q values. The curve of q-D_q is called the D_q spectrum.

$C_q\,(r)$ is calculated using equation 4 (b) for the epicentral distribution X_i, X_j of the subset. The distance r between two events is calculated using the spherical triangle method. For epicentral distributions having a fractal structure, the power-law relationship is obtained in the scaling region. An appropriate scaling region has to be estimated before the computation of the generalized dimension D_q. The scaling region is the linear segment in the graph of log r versus log $C_q\,(r)$.

The generalized dimension D_q is calculated for the consecutive fifty event time windows prior to the strong events, to see the temporal variation of D_q following the procedure outlined above.

3. Data

USGS PDE data ($m_b \geq 3$) has been used for the period January 1, 1973 to May 22, 2006 for the study of the region around Bam in southeastern Iran in search of numerical precursors of some of the devastating earthquakes in past years. The consecutive 30 windows formed for each 50 events totaling 1500 for the region within latitudes (24° N–34° N) and longitudes (54° E – 64° E). These data have also been analyzed taking 30 events at a time thereby forming 50 windows. The USGS PDE data ($m_b \geq 3$) has also been used for the period January 1,1973–May 23,2006 to study the region within latitudes (34° N–44° N) and longitudes (54° E–64° E). The consecutive 11 windows formed for each 50 events totaling 550 for the region within latitudes (34° N–44° N) and longitudes (54° E–64° E). USGS PDE data ($m_b \geq 3$) for the period January 1, 1973 to May 28, 2006 have been used to study the smaller region within latitudes (28° N–31° N) and longitudes (56° E–60° E). The 13 windows formed for each 30 events totaling 390. The

historical seismicity formed the basis of selecting our domain of analysis. The 50 events window is taken on the basis of detection of a sharp D_c anomaly prior to a large event in a reasonable time span for proper utility of this warning system for hazard mitigation. If the window size was taken 100 or 150 events which is usually done by many authors, it will render the detection of the precursor for a considerable longer time span and be less diagnostic. NAKAYA and HASHIMOTO (2002) indicate that in order to detect a more sensitive temporal variation of D_q within a shorter time span it is necessary to analyse time events over as shorter time period as possible. If we take less than 30 events window it becomes difficult to maintain the range of correlation coefficients of the regression line for the linear segment, which is considered for more than 0.97 in all the graphs of log r vs. log C_q (r) used for determining D_C and D_q. In general this analysis has to be done for an active tectonic setting to find the potential for a large earthquake. One has to start the analysis with a large spatial window (10° × 10°) for 30, 50, 100 etc. event time window and then re-analyse for a small spatial window (5° × 5°) for 30, 50, 100 etc., event time window until all possible spatio-temporal pattern of seismicity has been found. The scaling range for the linear portion of log r vs. log C_q (r) plot is about 5 km–90 km, which is well within the region of the study considered. The value of the scaling region is approximately smaller than $1/3 \sim 1/4$ of the side length of the analysis region complying with the study (HIRATA and IMOTO, 1991) ruling out a boundary effect on our analysis.

4. Results

The initial study of correlation fractal dimension of all events with $m_b \geq 3$ occurring in the south-eastern Iran region shows that its value fluctuates with time. D_C values have been plotted against mean time of each fifty-event windows as well as thirty-event windows for consecutive periods to study the variation of spatial correlation dimension with time. The correlation integral method is used to obtain the correlation fractal dimension and generalized fractal dimension. Hence we will obtain the spatio-temporal pattern of intermediate earthquakes prior to all the large earthquakes in the region.

In the region between latitudes (24° N–34° N) and longitudes (54° E–64° E) clustering was observed prior to the earthquake of M_w = 7.8, 16.9.1978. Several low D_c value of 1.2214 (for the window with mean time 10.4.1975); low D_c values of 1.2652 (for the window with mean time 23.7.1976) ; low D_c value of 1.2119 (for the window with mean time 24.12.1977) have been found while taking 50-event windows prior to the earthquake of $M_w = 7.8$, 16.9.1978 as shown in Figure 2 (c). Also several low D_c values of 1.0752 (for the window with mean time 13.3.1976); low D_c value of 1.3113 (for the window with mean time 19.6.1977); low D_c value of 1.1623 (for the window with mean time 9.4.1978) have been found while taking 30-event windows prior to the same earthquake of $M_w = 7.8$, 16.9.1978 as shown in Figure 2 (d).

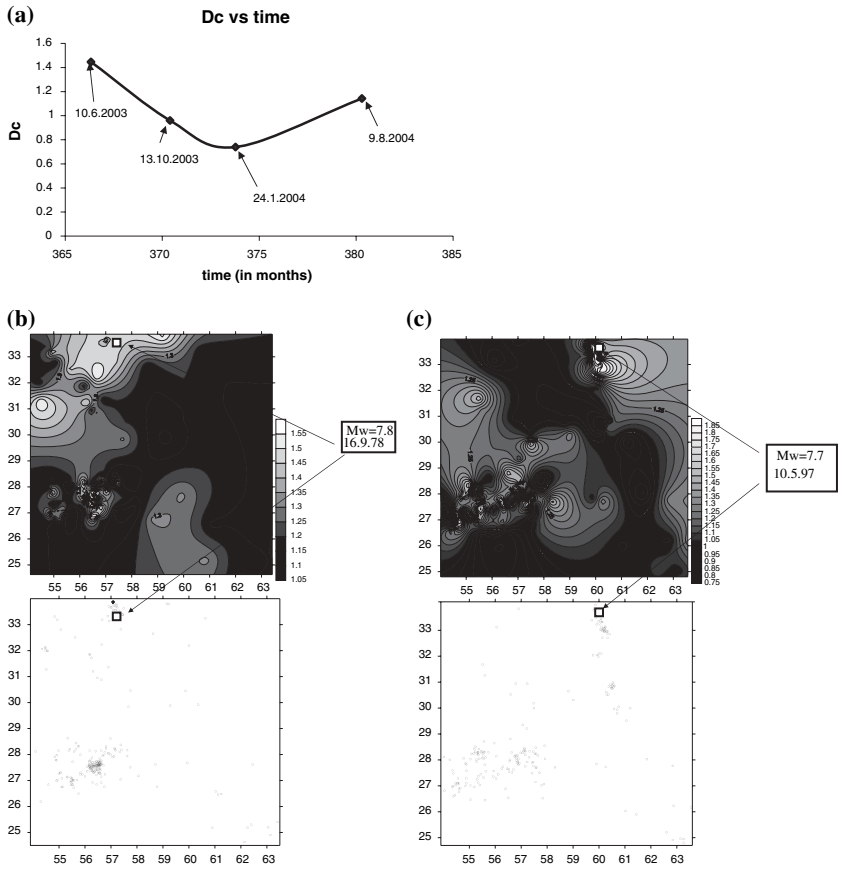

Figure 3

(a) : Considering event 26.12.2003 ($M_w = 6.8$) at latitude = 29° N and longitude = 58.31° E as a main shock. D_c value calculated and temporal variation of D_C are shown. The box of (13.10.2003) can be considered as a precursor of the event. (b) : Spatial distribution for the latitude (24° N–34° N) and longitude (54° E–64° E) of time windows of 30 events each with two low D_C values 1.0752 and 1.1623, estimated considering 16.9.78 ($M_w = 7.8$) as main event. Plotted contour with these two low D_C value patches represents the possible asperity or highly-stressed region. The second figure represents the spatial distribution of 30 events which fall in the low D_c value window showing clustering of the events. (c) : Spatial distribution for the latitude (24° N–34° N) and longitude (54° E–64° E) of time windows of 30 events each with two low D_C values 0.8278 and 0.9899, estimated considering 10.5.97 ($M_w = 7.7$) as main event. Plotted contour with these two low D_C value patches represents the possible asperity or highly-stressed region. The second figure represents the spatial distribution of 30 events which fall in the low D_c value window showing clustering of the events. (d) : Spatial distribution for the latitude (24° N– 34°N) and longitude (54° E–64° E) of time windows of 30 events, each with two low D_C values 0.7997 and 1.0317, estimated considering 26.12.2003 ($M_w = 6.8$) as main event. Plotted contour with these two low D_C value patches represents the possible asperity or highly stressed region. The second figure represents the spatial distribution of 30 events which fall in the low D_c value window showing clustering of the events. (e) : Spatial distribution for the latitude (24° N–34° N) and longitude (54° E–64° E) of time windows of 30 events each with three low D_C values 1.1513, 1.1737 and 0.6504 estimated considering the last eight time windows. Plotted contour with these two low D_C value patches represents the possible asperity or highly stressed region. The second figure represents the spatial distribution of 30 events which fall in the low D_c value window showing clustering of the events.

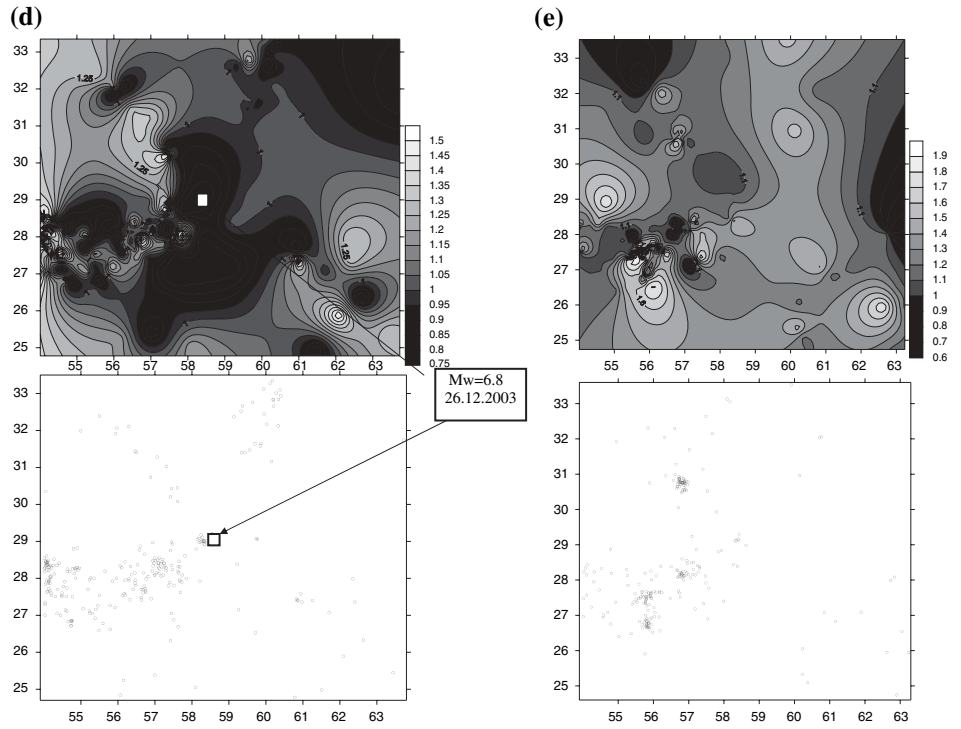

Figure 3
(Contd.)

Clustering was also observed prior to the earthquake of $m_b = 6.8$ on 26.12.2003 as shown in Figure 3 (a). A low D_c value of 0.9598 was estimated in the window with mean time 13.10.2003 using 30-event windows.

Clustering has also been observed in Figure 2 (c) with the last few windows showing a first low D_c value of 1.099 (for the window with mean time 19.6.2005) and second low D_c value of 0.7897 (for the window with mean time 13.3.2006) using 50-event windows. Similarly Figure 2 (d) indicates first low D_c value of 1.1737 (for the window with mean time 6.8.2005) , second low D_c value 1.0214 (for the window with mean time 10.2.2006), and a third low D_c value of 0.6504 (for the window with mean time 14.3.2006) which have also been estimated using 30-event windows which might indicate an impending major earthquake.

Generalized fractal dimension: The nature of slopes for Log C_q (r) – Log r obtained for the two consecutive time windows prior to the September 16, 1978 earthquake of $M_w = 7.8$ are shown in Figures 4 (a) and 4 (b). Similarly the nature of slopes for Log C_q (r) – Log r obtained for May 11, 1997 of $M_w = 7.7$ in Figures 4 (c) and 4 (d); December 26, 2003 of $M_w = 6.8$ in Figures 4 (e) and 4 (f); a possible impending earthquake in Figures 4 (g) and 4 (h). The range of r for which a plot of log C_q (r) against log (r) is a

Table 1

D_c and $D_2 - D_{22}$ values given for the region of latitude (24° N – 34° N) and longitude (54° E – 64° E) just prior to the event of Magnitude 7.8 (16.9.78)

Mean time/Date of windows	Events occurred	D_c values	$D_2 - D_{22}$ values
17.92889/28.5.74		1.1439	1.0878
32.22778/7.8.75		1.2024	1.1451
39.41889/13.3.76	**precursor**	**1.0752**	**1.0211**
50.72556/22.2.77		1.5557	1.4817
51.93222/28.3.77		1.5519	1.478
54.61444/19.6.77	Precursor	**1.3113**	**1.2488**
64.29444/9.4.78	**Precursor**	**1.1623**	**1.107**
70.39778/12.10.78	Mag. 7.8 (16.9.78)	1.4636	1.3939

straight line, is an indication of the range over which a fractal model holds. The D_q can be obtained from the linear portion of the plot Log $C_q(r)$ – Log r. The D_q obtained for different q is shown in the plot $D_q - q$ or D_q spectrum as shown in Figure 5(a) for September 16, 1978 of $M_w = 7.8$; Figure 5(b) for May 11, 1997 of $M_w = 7.7$; Figure 5(c) December 26, 2003 of $M_w = 6.8$ and Figure 5(d) for impending earthquakes. The $D_{2\text{-}22}$ values for the contributing significant low D_c value time windows are given in Tables 1–4. This can be, in other words, characterized as multifractal or heterogeneous fractal for the spatial distribution of events. This multifractal nature suggests that the events are showing cluster within cluster in the fractal structure. Further D_2–D_{22} variation with time shows a similar pattern before and after the main shock in Figures 5(e)–5(h) for the above earthquake. The variation of D_2–D_{22} for the foreshocks, as well as the aftershocks with time is in a fluctuating pattern. This variation can be explained assuming that asperity/barrier play a major role, which is controlling the strain in the tectonic stress field. The periodic variation is due to strain accumulation and liberation around the asperity/barrier.

Similarly, D_q are shown in Figures 5(i)–5(e) respectively, showing fluctuation between 0.65 and 1.85. The decrease and then increase of D_q with respect to the spatial distribution of seismic events indicate clustering and less clustering in multifractal

Table 2

D_c and $D_2 - D_{22}$ values given for the region of latitude (24° N – 34° N) and longitude (54° E – 64° E) just prior to the event of Magnitude 7.7 (10.5.97)

Mean time/Date of windows	Events occurred	D_c values	$D_2 - D_{22}$ values
235.4944/15.7.92		1.0148	0.9665
248.7744/24.8.93		1.0972	1.045
258.22/7.6.94	**Precursor**	**0.8278**	**0.7884**
269.9322/28.5.95		1.5432	1.4697
279.4/12.3.96	**Precursor**	**1.291**	**1.2296**
289.8844/27.1.97	**Precursor**	**0.9899**	**0.9427**
293.3378/11.5.97	Mag. 7.7 (10.5.97)	1.8184	1.7318

Table 3

D_c and $D_2 - D_{22}$ values given for the region of latitude (24° N – 34° N) and longitude (54° E – 64° E) just prior to the event of Magnitude 6.8 (26.12.03)

Mean time/Date of windows	Events occurred	D_c values	$D_2 - D_{22}$ values
316.1433/5.4.99		1.0183	0.9698
325.1578/5.1.00		0.9536	0.9082
334.9167/28.10.00	**Precursor**	**0.9285**	**0.8843**
344.0267/1.10.01	**Precursor**	**0.7997**	**0.7616**
351.38/12.3.02		1.1897	1.133
356.8933/27.8.02		1.298	1.2362
366.3256/10.6.03		1.5258	1.4532
370.4022/12.10.03	**Precursor**	**1.0317**	**0.9826**
373.7822/24.1.04	Mag. 6.8 (26.12.03)	0.7649	0.7285

Table 4

D_c and $D_2 - D_{22}$ values given for the region of latitude (24° N – 34° N) and longitude (54° E – 64° E) for the last 8 windows

Mean time/Date of windows	Events occurred	D_c values	$D_2 - D_{22}$ values
380.5344/16.8.04		1.1526	1.0977
386.1011/3.2.05		1.5105	1.4386
387.8678/26.3.05	**Precursor**	**1.1513**	**1.0965**
392.1756/6.8.05	**Precursor**	**1.1737**	**1.1254**
396.0367/2.12.05		1.5519	1.478
398.3333/10.2.06	**Precursor**	**1.0214**	**0.9727**
399.4589/14.3.06	**Precursor**	**0.6504**	**0.6021**
399.9311/27.3.06		1.8	1.7096

structure, respectively. The temporal variation of D_q reflects the accumulation and release of strain energy within the tectonic stress field. The variation of D_q for all the q values with respect to time has a similar nature to the earlier D_q and D_c plot.

5. Discussion and Conclusion

Most of Iran is located on a highland between the Zagros Mountains to the south and Arborz Mountains to the north. The highland consists of the continental crust of the Eurasian plate overlying the underthrusting Arabian plate. The collision-type plate boundary is considered to run along the southwestern foot of the Zagros Mountains northwest of the Hormuz Strait and along the Makran coast down to the triple junction in southern Pakistan (Fig. 1). The oblique convergence of Eurasian and Arabian plates results in right lateral and/or reverse slip on the intra-plate faults in southern Iran. The

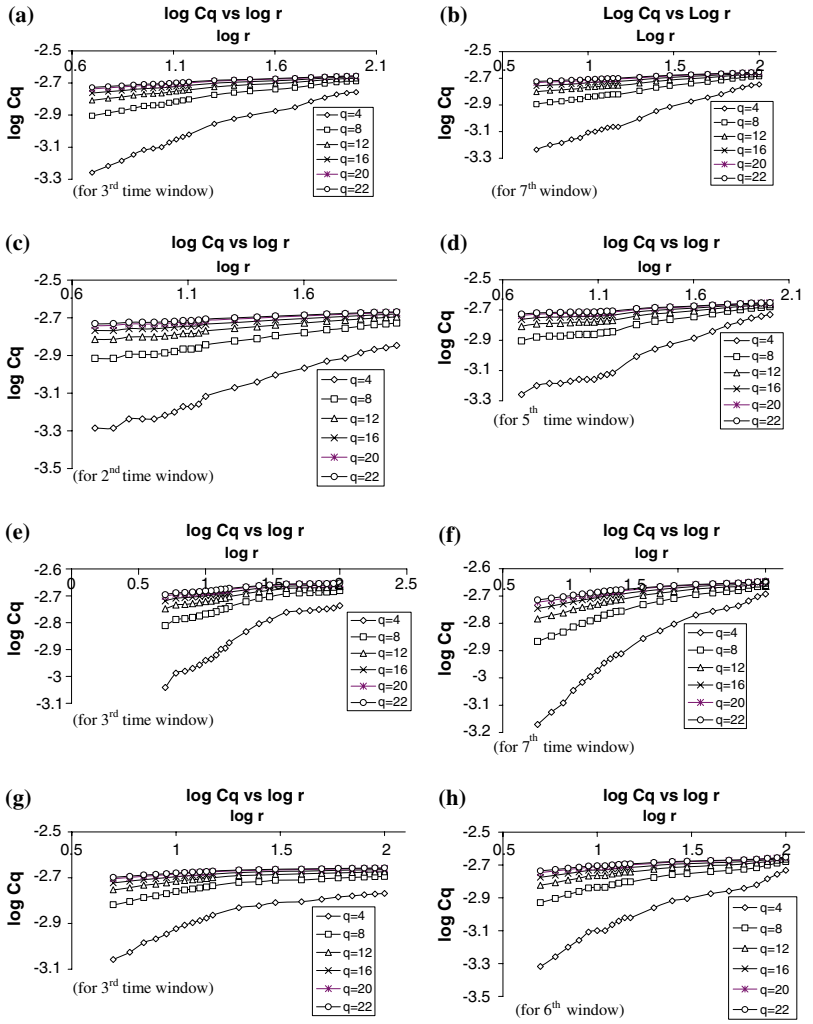

Figure 4

(a)–(b) : The log C_q (r) – log r relationship for spatial distribution of earthquakes for a window in the study. The slope of the linear portion of graph log C_q (r) – log r gives D_q for q = 4 to 22 for the event of magnitude M_w = 7.8 (16.9.78) within the region of study considered between latitude (24° N – 34° N) and longitude (54° E – 64°E). (c)–(d) : The log C_q (r) – log r relationship for spatial distribution of earthquakes for a window in the study. The slope of the linear portion of graph log C_q (r) – log r gives D_q for q = 4 to 22 for the event of magnitude M_w = 7.7 (10.5.97) within the region of study considered between latitude (24° N – 34° N) and longitude (54° E – 64° E). (e)–(f) : The log C_q (r) – log r relationship for spatial distribution of earthquakes for a window in the study. The slope of the linear portion of graph log C_q (r) – log r gives D_q for q = 4 to 22 for the event of magnitude M_w = 6.8 (26.12.03) within the region of study considered between latitude (24° N – 34° N) and longitude (54° E – 64°E). (g)–(h) : The log C_q (r) – log r relationship for spatial distribution of earthquakes for a window in the study. The slope of the linear portion of graph log C_q (r) – log r gives D_q for q = 4 to 22 for the last eight time windows within the region of study considered between latitude (24° N – 34° N) and longitude (54° E – 64° E).

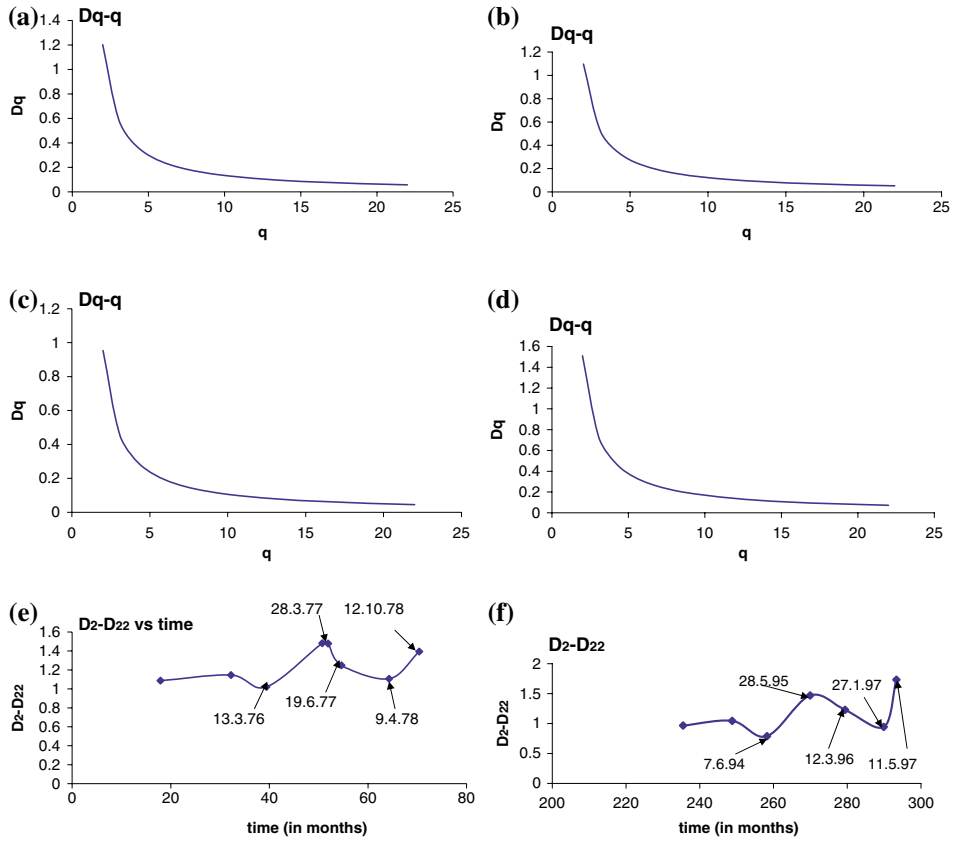

majority of the Quaternary and active faults here have a NW-SE to N-S strike, and show shortening with right-lateral slip (OKUMARA *et al.*, 2004).

Multifractal study with the correlation integral approach is necessary in order to quantify the spatial distribution with the help of generalized fractal dimension. Initially, the correlation- dimension was calculated with the correlation integral and it provided a point of view as to how the past events were mutually correlated. In other words it can be said that the correlation integral approach is a tool which helps to understand the cause of major events in the heterogeneous crust. The correlation dimension derived from the above approach reveals seismic clustering within the subdivisions of the study; the spatial fractal dimension D_2 varies from region to region. The short-term clustering is necessary to obtain the efficient and faithful model, where no practical results can be obtained from long-term effects. Hence a model is needed to explain the short-term, time-space-focal mechanism regularities of earthquake sequences (KAGAN, 1999). The correlation dimension derived from the above approach reveals the seismic clustering within the subdivisions of the study; the spatial fractal dimension D_2 varies from region to region. Analysis reveals significant variation in the multifractal properties of seismicity between

Figure 5

(a) : $D_q - q$ plot or D_q spectrum for second time window with $q = 2$ to 22. As the q value increases the exponential decay of D_q value shows the multifractal nature for the event of magnitude $M_w = 7.8$ within the region of study considered between latitude (24° N – 34° N) and longitude (54° E – 64° E). (b) : $D_q - q$ plot or D_q spectrum for second time window with $q = 2$ to 22. As the q value increases the exponential decay of D_q value shows the multifractal nature for the event of magnitude $M_w = 7.7$ within the region of study considered between latitude (24° N – 34° N) and longitude (54° E – 64° E). (c) : $D_q - q$ plot or D_q spectrum for second time window with $q = 2$ to 22. As the q value increases the exponential decay of D_q value shows the multifractal nature for the event of magnitude $M_w = 6.8$ (26.12.03) within the region of study considered between latitude (24° N – 34° N) and longitude (54° E – 64° E). (d) : $D_q - q$ plot or D_q spectrum for second time window with $q = 2$ to 22. As the q value increases the exponential decay of D_q value shows the multifractal nature for the last eight windows within the region of study considered between latitude (24° N – 34° N) and longitude (54° E – 64° E). (e) : The temporal variation of the difference $D_2 - D_{22}$ for spatial distribution of events ($M_L \geq 3$) for the event of magnitude $M_w = 7.8$ (16.9.78) within the region of study considered between latitude (24° N – 34° N) and longitude (54° E – 64° E). (f) : The temporal variation of the difference $D_2 - D_{22}$ for spatial distribution of events ($M_L \geq 3$) for the event of magnitude $M_w = 7.7$ (10.5.97) within the region of study considered between latitude (24° N – 34° N) and longitude (54° E – 64° E). (g) : The temporal variation of the difference $D_2 - D_{22}$ for spatial distribution of events ($M_L \geq 3$) for the event of magnitude $M_w = 6.8$ (26.12.03) within the region of study considered between latitude (24° N – 34° N) and longitude (54° E – 64° E). (h) : The temporal variation of the difference $D_2 - D_{22}$ for spatial distribution of events ($M_L \geq 3$) for the last eight windows within the region of study considered between latitude (24° N – 34° N) and longitude (54° E – 64° E). (i) : The temporal variation of multifractal dimension D_q for the spatial distribution of seismic events ($M_L \geq 3$) for the event of magnitude $M_w = 7.8$ (16.9.78) within the region of study considered between latitude (24° N – 34° N) and longitude (54° E – 64° E). (j) : The temporal variation of multifractal dimension D_q for the spatial distribution of seismic events ($M_L \geq 3$) for the event of magnitude $M_w = 7.7$ (10.5.97) within the region of study considered between latitude (24° N – 34° N) and longitude (54° E – 64° E). (k) : The temporal variation of multifractal dimension D_q for the spatial distribution of seismic events ($M_L \geq 3$) for the event of magnitude $M_w = 6.8$ (26.12.03) within the region of study considered between latitude (24° N – 34° N) and longitude (54° E – 64° E). (l) : The temporal variation of multifractal dimension D_q for the spatial distribution of seismic events ($M_L \geq 3$) for the last eight windows within the region of study considered between latitude (24° N – 34°N) and longitude (54° E – 64° E).

the tectonic subdivisions of the area under study. Difference between D_2 and D_{22} are related to differences in the tendency for seismicity to be clustered or dispersed at different scales. Hence the differences between the multifractal dimension D_2 and D_{22} are interpreted to result from fractal heterogeneity between regional and local scales, respectively (ÖNÇEL and WILSON, 2006). Changes between the fractal dimension D_c and multifractal (q = 2–22) measures illustrate the sensitivity of the multifractal characterization to changes in the local complexity. The marked difference between D_2 and D_{22} suggests the presence of significant 'fractal heterogeneity' within the hypocenter distribution of shallow seismicity due to differences in fault complexity at local scales i.e., q = 15, 16, …, 22. With the help of multifractal measures, the fractal properties of the complex fault system can be more suitably characterised.

In the study in southeastern Iran the D_c value varies between 0.7689 to 1.7834 for 50-event windows analysis; similarly it varied between 0.6504 to 1.8197 for 30-event windows analysis and it decreases just before the strong event. The decrease in this D_c value can be considered as a precursor for the future event. The significant low D_C value patch represents the possible asperity or highly stressed region and shows clustering of

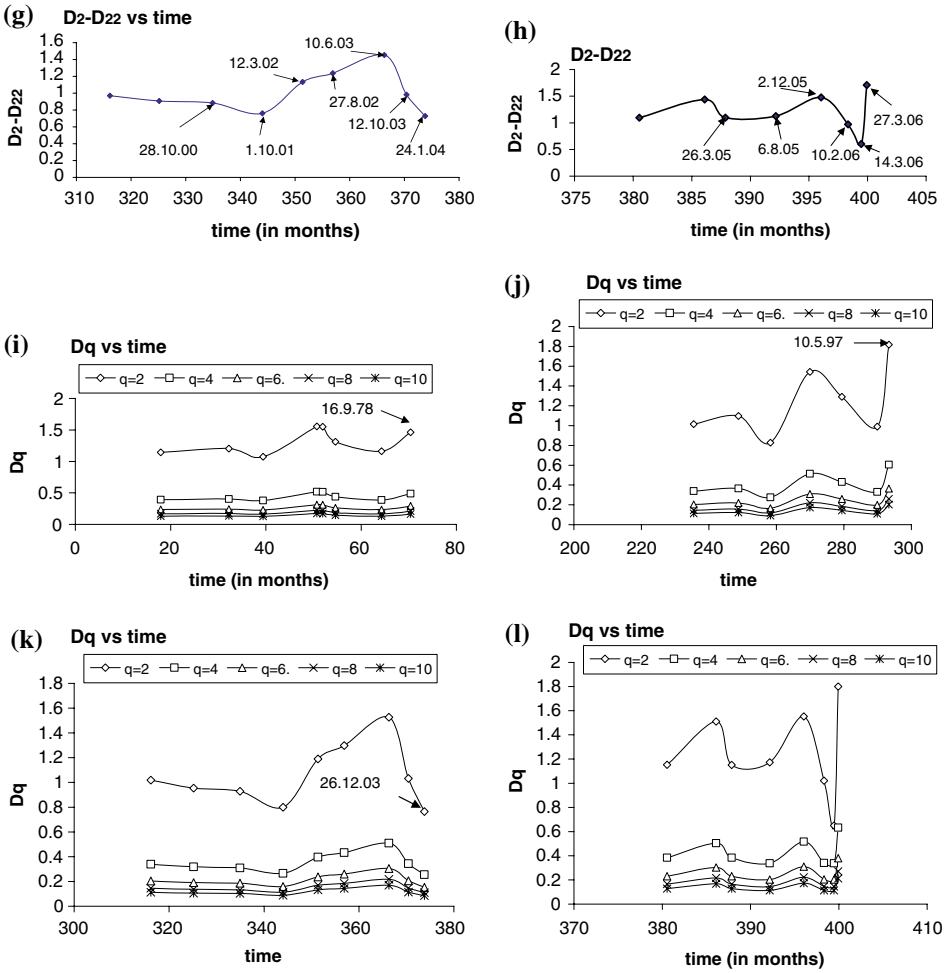

Figure 5
(Contd.)

the events indicated in Figures 3(b)–3(e). The difference between D_2 and D_{22} provides a direct measure of the complexity of the fault zone. The low mean value of D_2 and D_{22} for the region indicates towards the clustering of events. The D_q also shows a very low value, which varies with time. Firstly the increase of D_q value shows a declustering of events before the main event and then a sudden decrease in the D_q value prior to the release of a large amount of strain energy accumulated at an asperity. The major difference between (D_2 and D_{22}) suggests the presence of significant a fractal heterogeneity. Variations in the D_q response with q reveals the seismicity distribution is heterogeneous which has variable multifractal patterns of clustering in both space and time.

In the region lying between latitudes (24° N–34° N) and longitudes (54° E–64° E) the spatial fractal dimension D_2 varies between 1.0752 and 1.5557 and D_{22} varies between 0.0541 and 0.074 considering the event of magnitude 7.8 (16.9.78) as the main event. The periodical variation of D_q with time reflects the clustering of the events and strain energy accumulation prior to the main event of magnitude 7.8. The monotonous decrease of D_q over the range of q and periodical variation of (D_2–D_{22}) value at the same time until the large earthquake of this period occurs. These simultaneous phenomena indicate that the clustering in the spatial distribution of events developed over a wide range of q. The value of D_2 varies between 0.8278 and 1.8184 and D_{22} varies between 0.0394 and 0.0866 considering the event of magnitude 7.7 (10.5.97) as the main event. The gradual increase in the D_q and (D_2–D_{22}) with time reflects the process of slow accumulation of stress after which there occurs a decrease prior to the main event. The spatial fractal dimension D_2 varies between 0.7649 and 1.5258 and D_{22} varies between 0.0364 and 0.0726, considering the event of magnitude 6.8 (26.12.03) as the main event. The spatial fractal dimension D_2 varies between 0.6504 and 1.8 and D_{22} varies between 0.0483 and 0.0904, while considering the last eight time windows which show a possible precursor to a future major event. The variation of D_q with q reveals that the seismicity distribution is heterogeneous, consisting of variable multifractal patterns of clustering in both space and time. The approximate periodic variation of D_q and D_c with time suggests that the region has an asperity/barrier which controls the stress pattern. This kind of study can be helpful in understanding the cause of great earthquakes as well as the tool for future earthquake warning by examining the characteristic of D_q and D_c.

Tectonic processes generally activate the fault system where strain accumulation yields a highly stressed zone, i.e., an asperity. The rupture may nucleate from those weak zones accounting for most of the high frequency seismic energy radiation (TÖKSÖZ and NABELEK, 1984) eventually causing a large earthquake. The asperities are determined by the strength of the friction coefficient distribution over a fault zone that continues to trigger repeated earthquakes as controlled by fault surface heterogeneities. These zones interestingly possess different physical states and properties and hence can remain elusive from becoming mapped by various geophysical techniques. Imaging this intriguing nature of the sub-elements of the megathrusts is a challenge to be overcome by earth scientists.

The combined observational and simulation evidence suggests that the period of increased moment release in moderate earthquakes signals the establishment of long wavelength correlations in the regional stress field (JAUME and SYKES, 1999). The central hypothesis in the critical point model for regional seismicity is that it is only during these time periods that a region of the earth's crust is truly in or near a "self-organized critical" (SOC) state, such that small earthquakes cascade into much larger events. This may be attributed to self-similarity of earthquakes of different scales, which may allow fractures to self-organize in order to attain criticality as detected by the clustering of events at or in the immediate vicinity of the zone of asperity, ultimately causing the main shock. These clusterings can be monitored by the statistical precursor for the major earthquakes by considering a well-constrained earthquake catalogue of seismically active regions of the

world. SORNETTE and SAMMIS (1995) , SAMMIS *et al*. (1996), SALEUR *et al*. (1996a, b), and SAMMIS and SMITH (1999) also argue that the observed power-law buildings of intermediate events before a great earthquake represent the approach of the appropriate region toward a state of SOC.

Thus, in order to study the presence of asperity in the otherwise high seismic regime, the favorable condition for the release of accumulated strain accelerating seismic activity of moderate-sized earthquakes can, therefore, be assessed through the precursory spatio-temporal D_C variation study. The present work corroborates the earlier findings of OKUMURA *et al*. (2004) that the devastating event at Bam has not occurred in the past 700 years or more, and did not occur in, 2003, but it will occur in the future judging from the characteristics of the Bam fault. They are expecting a large, probably magnitude 7.5 or larger event, but they are unable to quantify the risks due to the unavailability of historic and geologic data. Figures 3(b) and 3(c) represent the D_C drops in the same area of high stress concentration, indicating the impending large earthquake. Although the events of magnitudes 7.8 (16.9.78) and 7.7 (10.5.97) are found to have occurred somewhat away from the region where the major clustering of events had taken place (Figures 3(b) and 3(c)) in spite of being in the 10° by 10° region of analysis considered for the study. This might be due to the oblique convergence of the Eurasian and Arabian plates.

Even KAGAN (1994, 1997) and MAIN (1995, 1996) discuss the advances in statistical analysis of seismological data, and new understanding of the scaling properties of seismicity: Possible universality of major properties of earthquake occurrence provides a unique opportunity to evaluate seismic hazard and to estimate the short- and long-term rate of future earthquake occurrence, i.e., to predict earthquakes statistically.

The significance of our findings is that D_C drops to significantly low values at several time windows prior to major earthquakes with specific mean times, if an analysis is performed on an earthquake catalogue of events for the period 1973–2006. To be very specific about this analysis and its importance can be judged by numerical warning rather than earthquake prediction. The occurrence of a large or great earthquake appears to dissipate a sufficient proportion of the accumulated regional strain to destroy these long wavelength stress correlations and bring the region out of an SOC state. Thus, this reproducible numerical precursor prior to major earthquakes, which is the indicator of an SOC state or asperity for different regions, might aid in better hazard mitigation and, therefore, disaster management for other seismically active regions experiencing past event episodes.

REFERENCES

AKI, K. (1981), *A probabilistic synthesis of precursory phenomena. earthquake prediction*, Amer. Geophys. Union, Washington. pp. 556–574.

AKI, K. (1984), *Asperities, barriers, characteristic earthquakes and strong motion prediction*, J. Geophys. Res. *89*, 5867–5872.

BERBERIAN, M. and YEATS, R.S. (1999), *Patterns of historical earthquake rupture in Iranian plateau*, Bull. Seismol. Soc. Am. *89 (1)*, 120–139.

BUNDE, A., HAVLIN, S., and ROMAN, H. E. (1990), *Multifractal features of random walks on random fractals*, Phys. Rev. A *42*, 6274.

FENG, X. T. and SETO, M. (1999), *Fractal structure of the time distribution of microfracturing in rocks*, Geophys. J. Int. *136*, 275–285.

FIELDING, E.J., TALEBIAN, M., ROSEN, P.A., NAZARI, H., JACKSON, J.A., GHORASHI, M., and WALKER, R. (2005), *Surface rupture and building damage of the 2003 Bam, Iran, earthquake mapped by satellite synthetic aperture radar interferometric correlation*, J. Geophys. Res. *110*, B03302, doi:10.1029/2004JB003299.

GRASSBERGER, P. and PROCCACIA, I. (1983), *Characterizations of stranger attractors*, Phys. Rev. Lett. *50*, 346–349.

HALSEY, T.C., JENSON, M.H., KADANOFF, L.P., PROCACCIA, I., and SHRAIMAN, B.I. (1986), *Fractal measure and their singularities: The characterization of strange sets*, Phys. Rev. A *33 (2)*, 1141–1151.

HILAROV, V.L. (1998), *Self-similar crack-generation effects in the fracture process in brittle materials*, Modelling Simul. Mater. Sci. Eng. *6*, 337–342.

HIRATA, T., (1989), *Fractal dimension of fault systems in Japan: Fractal structure in rock fracture geometry at various scales*, Pure Appl. Geophys. *131*, 157–170.

HIRATA, T. and IMOTO, M. (1991) , *Multifractal analysis of spatial distributions of microearthquake in the Kanto Region*, Geophys. J. Int. *107*, 155–162.

ITO, K. and MATSUZAKI, M. (1990). *Earthquakes as self-organized critical phenomena*, J. Geophys. Res. *95*, 6853–6860.

JAUME, S. C. and SYKES, L. R. (1999), *Evolving towards a critical point: A review of accelerating seismic moment/energy release prior to large and great earthquakes*, Pure Appl. Geophys. *155*, 279–306.

KAGAN, Y. Y. (1994), *Observational evidence for earthquakes as a nonlinear dynamic process*, Physica D *77*, 160–192.

KAGAN, Y. Y. (1997), *Are earthquake predictable?* Geophys. J. Int. *131*, 505–525.

KAGAN, Y. Y. (1999), *Is earthquake seismology a hard, quantitative science?* Pure Appl. Geophys. *155*, 233–258.

KING, G. (1983), *The accommodation of large strains in the upper lithosphere of the earth and other solids by self-similar fault system: The geometrical origin of b-value*, Pure Appl. Geophys. *121*, 761–815.

LEGRAND, D., CISTERNAS, A., and DORBATH, L. (1996), *Multifractal analysis of the 1992 Erzinçan aftershock sequence*, Geophy. Res. Lett. *23 (9)*, 933–936.

MAIN, I. G. (1995), *Earthquake as critical phenomena-implication for probabilistic seismic hazard analysis*, Bull. Seismol. Soc. Am. *85*, 1299–1308.

MAIN, I. G. (1996), *Statistical physics, seismogenesis and seismic hazard*, Rev. Geophys. *34*, 433–462.

MANDAL, P., MABAWONKU, A. O., and DIMRI V. P. (2005), *Self-organized fractal seismicity of reservoir triggered earthquakes in the Koyna-Warna seismic zone, Western India*, Pure Appl. Geophys. *162*, 73–90.

MANDELBROT, B.B. (1989) , *Multifractal measures: Especially for the geophysist*, Pure Appl. Geophys. *131 (l/2)*, 5–42.

NAKAYA, S. and HASHIMOTO, T. (2002), *Temporal variation of multifractal properties of seismicity in the region affected by the mainshock of the October 6, 2000 Western Tottori prefacture, Japan, earthquake (M = 7.3)*, Geophys. Res. Lett. *29*, 133-1-133-4.

OKUMARA, K., KONDO, H., AZUMA, T., ECHIGO, T., and HESSAMI, K. (2004), *Surface effects of the December, 26th, 2003 Bam earthquake along the Bam fault in southeastern Iran*, Bull. Earthq. Res. Inst., Univ. Tokyo *79*, 29–36.

ÖNÇEL, A. O., ALPTEKIN, O., and MAIN, I. (1995), *Temporal variations of the fractal properties of seismicity in the western part of the north Anatolian fault zone: Possible artifacts due to improvements in station coverage*, Nonlinear Processes in Geophys. *2*, 147–157.

ÖNÇEL, A. O. and WILSON, T.H. (2002), *Space-Time correlations of seismotectonic parameters: Example from Japan and from Turkey preceding the Izmith earthquake*, Bull. Seismol. Soc. Am. *92*, 339–349.

ÖNÇEL, A.O. and WILSON, T. (2004), *Correlation of seismotectonic variables and GPS strain measurements in western Turkey*, J. Geophys. Res. *109*, B11306.

ÖNÇEL, A.O. and WILSON, T. (2006), *Evaluation of earthquake potential along the northern Anatolian Fault zone in the Marmara Sea using comparisons of GPS strain and seismotectonics parameters*. Tectonophysics *418*, 205–218.

PAWELZIK, K. and SCHUSTER, H.G. (1987), *Generalized dimensions and entropies from a measured time series*, Phys. Rev. *35*, 481–484.

ROY, P. N. S. and RAM, A. (2006), *A correlation integral approach to the study of 26 January 2001 Bhuj earthquake, Gujarat, India*, J. Geody. *41*, 385–399.

SALEUR, H., SAMMIS, C.G., and SORNETTE, D. (1996a), *Discrete scale invariance, complex fractal dimensions, and log-periodic fluctuations in seismicity*, J. Geophys. Res. *101*, 17,661–17,677.

SALEUR, H., SAMMIS, C.G., and SORNETTE, D. (1996b), *Renormalization group theory of earthquakes*, Nonlinear Processes in Geophys. *3*, 102–109.

SAMMIS, C. G. and SMITH S. W. (1999), *Seismic cycles and the evolution of stress correlation in cellular automation models of finite fault networks*, Pure Appl. Geophys. *155*, 307–334.

SAMMIS, C. G., SORNETTE, D., and SALEUR, H. (1996), *Complexity and earthquake forecasting, reduction and predictability of natural disasters, SFI studies in the science of complexity*, vol. XXV (eds. J. B. Rundle, W. Klein, and D.L. Turcotte) (Addison-Wesley, Reading, Mass. 1996) pp. 143–156.

SHOJA-TAHERI, J. and NIAZI, M. (1981), *Seismicity of the Iranian plateau and bordering regions*, Bull. Seismol. Soc. Am. *71 (2)*, 477–489.

SORNETTE, D. and SAMMIS, C.G. (1995), *Complex critical exponents from renormalization group theory of earthquakes: Implications of earthquake predictions*, J. Phys. *22*, 411–414.

STANLEY, H.E. and MEAKIN, P. (1988), *Multifractal phenomena in physics and chemistry*, Nature *335*, 405.

TALEBIAN, M. *et al*. (2004). *The Bam (Iran) earthquake: rupture of a blind strike slip fault*, Geophys. Res. Lett. *68 (1)*,199–222.

TEOTIA, S. S., KHATTRI, K.N., and ROY, P.K. (1997), *Multifractal analysis of seismicity of the Himalyan region*, Current Science *73*, 359–366.

WALKER, R. and JACKSON, J.A. (2002), *Offset and evolution of the Gowk fault, S.E.Iran: A major intra-continental strike-slip system*., J. Struct. Geol. *24*, 1677–1698.

WIEMER, S. and WYSS, M. (2000), *Minimum magnitude of completeness in earthquake catalogs: Example from Alaska, the Western United States, and Japan*, Bull. Seismol. Soc. Am. *90*, 859–869.

(Received January 5, 2007, accepted April 24, 2007)